Unsupervised Generalizable Multi-source Person Re-identification: A Domain-specific Adaptive Framework

Lei Qia, Jiaqi Liua, Lei Wangb, Yinghuan Shic, Xin Genga,*

^aSchool of Computer Science and Engineering, Southeast University, Nanjing, China ^bSchool of Computing and Information Technology, University of Wollongong, Wollongong, Australia ^cState Key Laboratory for Novel Software Technology, Nanjing University, Nanjing, China

Abstract

Domain generalization (DG) has attracted much attention in person re-identification (ReID) recently. It aims to make a model trained on multiple source domains generalize to an unseen target domain. Although achieving promising progress, existing methods usually need the source domains to be labeled, which could be a significant burden for practical ReID tasks. In this paper, we turn to investigate "unsupervised" domain generalization for ReID, by assuming that no label is available for any source domains. To address this challenging setting, we propose a simple and efficient domain-specific adaptive framework, and realize it with an adaptive normalization module designed upon the batch and instance normalization techniques. In doing so, we successfully yield reliable pseudo-labels to implement training and also enhance the domain generalization capability of the model as required. In addition, we show that our framework can even be applied to improve person ReID under the settings of supervised domain generalization and unsupervised domain adaptation, demonstrating competitive performance with respect to relevant methods. Extensive experimental study on benchmark datasets is conducted to validate the proposed framework. A significance of our work lies in that it shows the potential of unsupervised domain generalization for person ReID and sets a strong baseline for the further research on this topic. The code is available at https://github.com/Qi5Lei/DSAF.

^{*}Corresponding author: Xin Geng.

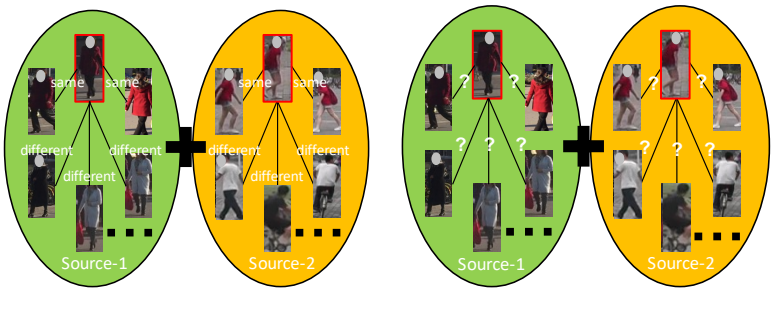
Email addresses: qilei@seu.edu.cn (Lei Qi), liu_jq@seu.edu.cn (Jiaqi Liu), leiw@uow.edu.au (Lei Wang), syh@nju.edu.cn (Yinghuan Shi), xgeng@seu.edu.cn (Xin Geng)

1. Introduction

Person re-identification (ReID) is to match different images of one identity from the non-overlapping cameras in a video-surveillance system. The key is to obtain the discriminative feature to distinguish the same or different identities [1, 2, 3, 4]. The challenges of ReID involve the variation on views, illumination, background, resolution, etc. of different cameras. Many methods have been developed for this task. Thanks to the power of deep learning, person ReID has been well addressed in the supervised case [5, 6, 7, 8, 9, 10, 11].

Recently, person ReID has been expanded to consider other settings. Unsupervised domain adaptation (UDA) methods are developed [12, 13, 14, 15, 16, 17, 18, 19], with the goal of making a ReID model trained on a labelled source domain work effectively on a given target domain. Also, domain generalization (DG) has attracted much attention in person ReID [20, 21, 22]. It aims to make a model trained on multiple labeled source domains generalize to an unseen target domain. Both settings, particularly DG, considerably expand the application scope of person ReID in practice. However, existing UDA and DG methods still require source domains to be labeled in advance in order to train the model. It is well known that obtaining label information for person ReID is labor-expensive and time-consuming.

In this paper, we attempt a more challenging task, named unsupervised domain generalization ReID (UDG-ReID), *i.e.*, unsupervised generalizable multi-source person re-identification. It is assumed that all label information of source domains becomes unavailable in the training stage, while the target domain remains unseen during training. Compared to the typical DG-ReID, our setting, as shown in Fig. 1, removes the cost of data labeling in real-world applications. Besides, different from UDA, our task is now to exploit multiple unlabeled source domains and enhance the generalization ability of the model in an unseen domain, and is therefore more difficult than the UDA-ReID case. Tab. 1 highlights the key differences among these tasks.



(a) Typical setting (Supervised)

(b) Our setting (Unsupervised)

Figure 1: Comparison between the settings of typical DG-ReID and our unsupervised DG-ReID. As seen, in our task, all source domains have no label information in the training stage. Note that we use two unlabeled source domains just as an example here. The testing domain is unseen in the two tasks, as shown in Tab. 1.

Table 1: Comparison of different ReID tasks. "ASL" and "ATD" indicate the "available source labels" and the "available target domain" during training, respectively.

Task	ASL (Y/N)	ATD (Y/N)
UDA-ReID	✓	✓
UDAw/oSL-ReID (ours)	×	✓
DG-ReID	✓	Х
UDG-ReID (ours)	×	×

For the proposed UDG-ReID task, two issues have to be addressed. Firstly, compared to UDA-ReID, which only needs to generate pseudo-labels for one target domain, we need to do this for multiple unlabeled source domains during the training course. Particularly, since there exists domain-shift between different source domains, the generation of pseudo-labels for unlabeled data therein will unavoidably be disturbed. In this case, the common practice of using a shared network path to extract the features for all source domains will not be appropriate anymore, as will be shown in Fig. 3 of Sec. 3.2 shortly. Secondly, in the training stage, we still need to attend to the generalization ability of the model with respect to unseen target domain, as existing DG methods do. When there is a significant domain gap between source and target domains, the model trained on the source domains will not work well in the target domain.

In this paper, we address the above two issues in a unified framework. To this end,

a domain-specific adaptive framework (DSAF) is proposed for the UDG-ReID task. Specifically, to reduce the impact of domain shift on pseudo-label generation, we create a domain-specific network path for each of the source domains, so as to achieve more accurate pseudo-label prediction. At the same time, to obtain good generalization ability on unseen target domain, we create another path to adaptively mitigate the domain gap between the multiple source domains and the unseen target domain. Following the design, this work realizes the proposed framework via the normalization techniques in deep learning. This produces the domain-specific adaptive normalization (DSAN) which will become clear shortly.

We conduct experiments on multiple benchmark datasets to show the potential of our method. Besides, we demonstrate that our method can also be adapted to supervised DG-ReID setting and outperform existing methods. Furthermore, motivated by the proposed UDG-ReID, we introduce another new setting called UDA without source labels (UDAw/oSL), as shown in Tab. 1. Although requiring no labels in source domain, with our method, it can yield competitive performance versus existing UDA-ReID methods. Our contributions are summarized as below:

- We propose an unsupervised domain generalization person ReID (UDG-ReID)
 task in the person ReID community. It does not need label information for source
 domains, and is therefore more challenging but practical than typical DG-ReID
 task.
- We develop a simple yet effective domain-specific adaptive framework to reduce the adverse impact of domain gap across source domains during generating pseudo-labels and boost the generalization ability of the model for the unseen target domain.
- We evaluate our method on multiple benchmark datasets. The results show that
 it achieves higher accuracy than baselines on all datasets. Besides, our method
 adapted to supervised DG-ReID task and the new task of UDA without source
 labels also demonstrates promising performance.

The rest of this paper is organized as follows. We review some related work in

Section 2. The proposed method is introduced in Section 3. Experimental results and analysis are presented in Section 4, and Section 5 is conclusion.

2. Related Work

In this section, we review some related works to our work in the following part, including supervised domain generalization (DG) person ReID and unsupervised domain adaptation (UDA) person ReID.

2.1. Supervised DG Person ReID

Some existing DG-ReID methods aim to learn the domain-invariant feature for any domain. Jia *et al.* [23] observe that appropriate instance and feature normalization alleviates style and content variance across datasets in deep ReID models. Jin *et al.* [24] propose to distill the identity-relevant feature from the information removed by instance normalization (IN) [25] and restore it to the network to ensure high discrimination. Zhao *et al.* [26] develop the memory-based multi-source meta-learning framework to train a generalizable model for unseen domains. In [20], a novel deep ReID model termed domain-invariant mapping network is proposed, which can learn a mapping between a person image and its identity classifier.

In addition, some methods employ the adaptive technique to make the trained model better generalize in the unseen target domain. The method [27] treats image matching as finding local correspondences in feature maps and constructs query-adaptive convolution kernels on the fly to achieve local matching. To generalize normalization layers, this work [21] combines learnable batch-instance normalization layers with meta-learning. Differently, in [22], a voting-based mixture mechanism is used to dynamically leverage diverse characteristics of source domains, which can better improve the generalization ability of models. Compared to the supervised DG person ReID, there is no available label information in the training stage in our task, *i.e.*, we do not know the label of the source domain, as shown in Tab. 1.

In our UDG-ReID task, we not only need to learn the robust model in the unseen domain, but also reduce the interference of domain gap between unlabeled source domains to produce the better pseudo-labels. In addition, several DG methods have also obtained great success in the classification task and the semantic segmentation task [28, 29, 30, 31, 32, 33]. For example, Nam *et al.* [34] propose to reduce the intrinsic style bias of CNNs to close the gap between domains. Considering that the Fourier phase information contains high-level semantics and is not easily affected by domain-shift, Xu *et al.* [35] introduce a novel Fourier-based perspective for domain generalization. Seo *et al.* [36] develop a simple but effective multi-source domain generalization technique based on deep neural networks by incorporating optimized normalization layers that are specific to individual domains. However, most of these methods do not also need to tackle the case without the labels of all source domains.

2.2. UDA Person ReID

As mentioned in Sec. 1, our task is also related to the UDA-ReID case. Most of the successful UDA-ReID methods use clustering-based pseudo-label prediction with representation learning and perform the two steps in an alternating fashion [37, 38, 39, 40, 41, 42, 43, 44]. However, because of the domain gap, the pseudo-labels from the model trained in the source domain are not always reliable and there are incorrect labels. Most of existing methods mainly aim to alleviate the negative effects of noisy labels.

In [45], a dynamic and symmetric cross-entropy loss is developed to deal with noisy samples and accommodate to the change of clusters. Zheng *et al.* [46] estimate and exploit the credibility of the assigned pseudo-label of each sample by suppressing the contribution of noisy samples. Differently, Ge *et al.* [47] propose to softly refine the pseudo-labels in the target domain by proposing an unsupervised framework to learn better features from the target domain via off-line refined hard pseudo-labels and online refined soft pseudo-labels in an alternative training manner. The method in [48] enables the online interaction and mutual promotion of pseudo-label prediction and representation learning to better correct the noisy labels.

Besides, Xuan *et al.* [49] split the sample similarity into the intra-camera and inter-camera computations, respectively, which effectively alleviates the distribution gap among cameras to generate more reliable pseudo-labels. In particular, most of the

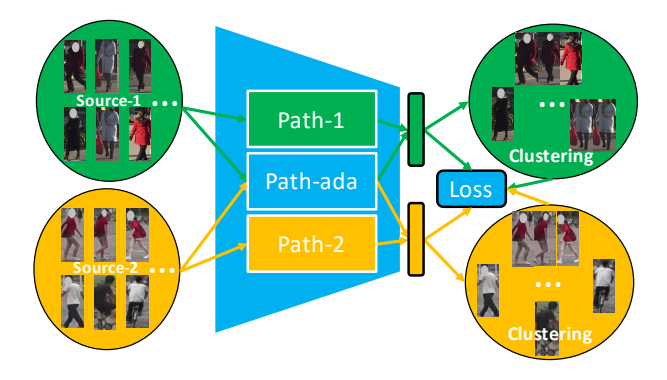


Figure 2: Overview of the proposed DSAF. Note that we take two unlabeled source domains as an example in this figure. In the framework, the independent path for each domain is to alleviate the impact of the interdomain interference during the pseudo-label generation. The "path-ada" is to boost the generalization ability in the unseen target domain.

existing pseudo-label-based methods mainly aim to produce the pseudo-label for an unsupervised domain. Differently, in our task, all domains in the training stage are unlabeled, hence we aim to alleviate the impact of the inter-domain interference during the pseudo-label generation. In [50], a novel self-paced contrastive learning framework is proposed to exploit all valuable information. Moreover, to use the valuable labeled data, a rectification domain-specific batch normalization module is introduced for the multi-source UDA-ReID in [51].

These aforementioned methods try to handle the case without the labels of the target domain. However, unlike the UDA-ReID task, in our UDG-ReID task, the target domain cannot be seen in the training stage, and all source domains do not include the label information, as shown in Tab. 1.

3. Methodology

In this section, we firstly introduce the unsupervised domain generalization person ReID (UDG-ReID). Then, we present the proposed domain-specific adaptive framework (DSAF). Moreover, we describe the domain-specific adaptive normalization (DSAN). Finally, we give the details of the network.

3.1. Unsupervised Domain Generalization Person ReID

Recently, an unsupervised domain generalization (UDG) task has been proposed for the classification task [52], which can be considered as a self-training task [53, 54] with the domain-shift in the training samples, *i.e.*, training a pre-trained model. It is worth noting that, the UDG task for classification needs a few labeled images in the target domain. The main reason is that the pre-trained model cannot predict which class an image belongs to, thus a few labeled images from the target domain are required to train the classifier or fine-tune the pre-trained model. Therefore, the UDG for classification is not a strict domain generalization (DG) task.

Differently, person ReID is a metric task, which aims to learn the discriminative features to evaluate the similarity between different images, *i.e.*, it does not require predicting which ID an image belongs to. Particularly, the current existing tasks for mitigating the requirement of labeling or collecting data in the person ReID mainly include the UDA and DG. For the UDA task, it still needs to collect data from the target domain, while the DG task requires the labeled data in the training stage. To further alleviate this issue, we propose an unsupervised domain generalization Re-ID task, where there is no label information for the training data and the labeled images of the target domain are not required during testing. In our task, assuming that we have N_d domains ($\{D_1, D_2, \dots, D_{N_d}\}$) without labels to train the network, we aim to output a generalizable model $\hat{\theta}$ to the unseen domain.

It is worth noting that the difference between our setting and domain-incremental learning [55, 56] is the definition of the domain. In domain-incremental learning, all domains belong to the same dataset, while all classes in each domain are not overlapping, *i.e.*, the distribution of the **output** is different. In contrast, in our setting, each domain belongs to different datasets, *i.e.*, the distribution of the **input** is different.

3.2. Domain-Specific Adaptive Framework

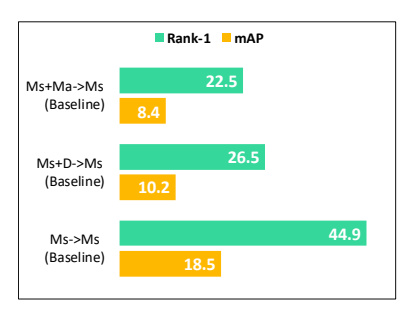
For the proposed unsupervised domain generalization person ReID (UDG-ReID), there are two key problems as below: 1) there is no label information in all source domains, and 2) the target domain could be different from all source domains from

the data-distribution perspective. Therefore, most of existing DG-ReID or UDA-ReID methods cannot be directly applied to deal with the UDG-ReID.

For the former issue, in the UDG-ReID task, we need to generate the pseudo-labels for all source domains, thus the discriminative feature representation is required for each unlabeled sample. However, since there is the domain gap between different source domains, if we utilize a completely shared path for all source domains in the backbone network during training, each domain will be disturbed each other during pseudo-labeling. As shown in Fig. 3 (a), the model trained on the MSMT17 dataset can obtain a better performance than the model jointly trained on MSMT17 and other datasets when evaluated on MSMT17. It is worth noting that we do not provide the label information for all training samples in the experiment. Besides, we report the clustering evaluation of unlabeled training data on MSMT17, as shown in Fig. 3 (b), and there is the similar pattern to Fig. 3 (a). This reveals that jointly training model using multiple unlabeled datasets (*i.e.*, domains) reduces the robustness of features due to the domain gap between different training domains, which decreases the reliability of pseudo-labels. Therefore, for UDG-ReID, we need to deal with this issue.

For the latter issue, the generalization ability of the model is key for the unseen target domain due to the domain gap between source and target domains. Most of the existing methods aim to improve the robustness of the model by learning the domain-invariant feature or conducting the augmentation operation on the features or images. Particularly, different from the conventional DG task, we aim to simultaneously consider the discrimination ability and the generalization ability of a model in the UDG-ReID task because of no available labels in all source domains.

In this paper, we propose a domain-specific adaptive framework (DSAF) to solve the above issues, as shown in Fig. 2. In this framework, we use the private path for each unlabeled source domain, which alleviates the impact of the inter-domain interference during the pseudo-label generation. Besides, we employ an adaptive path to boost the generalization ability in the unseen target domain, *i.e.*, a sample-adaptive path in the testing stage, which can remove the impact of the domain gap between sources domains and the unseen target domain when we extract features from the unseen domain. Finally, we fuse the features from the domain-specific path and the global adaptive





(a) Performance

(b) Clustering evaluation

Figure 3: Experimental results of different settings using the raw ResNet-50, *i.e.*, the baseline network in this paper, on MSMT17 (Ms). Note that "Ms+Ma→Ms" is that training the model on "Ms" and "Ma" (Market-1501), and evaluating the model on "Ms". Besides, "D" is DukeMTMC-reID in this figure. AMI (Adjusted Mutual Information) and FMI (Fowlkes-Mallows Index) [57] are two clustering evaluation protocols, and the larger value is better. Note that there are no available labels in the experiment.

path to conduct the clustering operation, and then generate pseudo-labels to train the model. After each epoch, we utilize the clustering algorithm to regenerate the new pseudo-labels.

3.3. Domain-Specific Adaptive Normalization

Since there is the domain gap between different domains, the statistics of batch normalization (BN) from different domains in the neural network are different. Therefore, domain-specific batch normalization (DSBN) [58] is proposed to alleviate the domain-shift between source and target domains in the classical UDA task. Besides, the instance normalization (IN) can enhance the generalization ability of the model by removing the style information with the sample-adaptive statistics in the DG task [23]. In this paper, inspired by these above methods, we develop a domain-specific adaptive normalization (DSAN) to achieve the proposed DSAF from the normalization perspective, which can simultaneously mitigate the interference between different source domains during generating pseudo-labels and boost the generalization ability in the unseen target domain in the unified framework, as illustrated in Fig. 4. In DSAN, DSBN and IN achieve the domain-specific path and the domain-adaptive path of DSAF in Fig. 2, respectively. Inspired by IBN-Net [59], we use a half feature maps into IN and

another feature maps to conduct the domain-specific BN, and then utilize the concat operation to fuse them. Given an example from domain d, its feature maps can be defined as $f_d \in \mathbb{R}^{N \times C \times H \times W}$, where H and W indicate spatial dimensions, and C and N are the number of channels and batch size. We split f_d into two parts according to channel dimension, $f_d = f_d^1 \oplus_c f_d^2$, where $f_d^1, f_d^2 \in \mathbb{R}^{N \times C/2 \times H \times W}$, and \oplus_c represents the concat operation based on the channel dimension. Thus, the global IN and the BN for the d-th domain can be formulated as:

$$IN(f_d^1; \gamma^{in}, \beta^{in}) = \gamma^{in} \frac{f_d^1 - \mu_n}{\sigma_n} + \beta^{in}, \tag{1}$$

$$BN_{d}(f_{d}^{2}; \gamma_{b}^{bn}, \beta_{b}^{bn}) = \gamma_{d}^{bn} \frac{f_{d}^{2} - \mu_{d}}{\sigma_{d}} + \beta_{d}^{bn}, \ d \in \{1, ..., D\},$$
 (2)

where $\gamma^{in}, \beta^{in}, \gamma^{bn}_d, \beta^{bn}_d \in \mathbb{R}^{C/2}$ are learnable affine transformation parameters, and D is the number of domains. μ_n, σ_n and $\mu_d, \sigma_d \in \mathbb{R}^{C/2}$ represent the channel-wise mean and standard deviation of IN and BN of each feature map as follows:

$$\mu_n = \frac{1}{HW} \sum_{h=1}^{H} \sum_{w=1}^{W} f_d^1[n,:,h,w], \tag{3}$$

$$\mu_d = \frac{1}{NHW} \sum_{n=1}^{N} \sum_{h=1}^{H} \sum_{w=1}^{W} f_d^2[n,:,h,w], \tag{4}$$

$$\sigma_n = \sqrt{\frac{1}{HW} \sum_{h=1}^{H} \sum_{w=1}^{W} (f_d^1[n,:,h,w] - \mu_n)^2 + \epsilon},$$
 (5)

$$\sigma_d = \sqrt{\frac{1}{NHW} \sum_{n=1}^{N} \sum_{h=1}^{H} \sum_{w=1}^{W} (f_d^2[n, :, h, w] - \mu_d)^2 + \epsilon},$$
 (6)

where ϵ is a constant for numerical stability. Therefore, our domain-specific adaptive normalization is defined as:

$$\hat{f}_d = DSAN(f_d) = IN(f_d^1; \gamma^{in}, \beta^{in}) \oplus_c$$

$$BN_d(f_d^2; \gamma_b^{in}, \beta_b^{in}), \quad d \in \{1, ..., D\}.$$
(7)

According to the above description, the forward process of the proposed DSAN is summarized in Algorithm 1.

Algorithm 1 The forward process of DSAN

- 1: Input: Give the d-th domain feature $f_d \in \mathbb{R}^{N \times C \times H \times W}$.
- 2: **Output:** The normalized feature \hat{f}_d .
- 3: Evenly split f_d into f_d^1 and f_d^2 on channel dimension.
- 4: Conduct instance normalization for f_d^1 with the shared affine transformation as Eq. (1), output \hat{f}_d^1 .
- 5: Conduct batch normalization for f_d^2 with the private affine transformation for the d-th domain as Eq. (2), output \hat{f}_d^2 .
- 6: Concat \hat{f}_d^1 and \hat{f}_d^2 on channel dimension to generate the normalized feature \hat{f}_d .

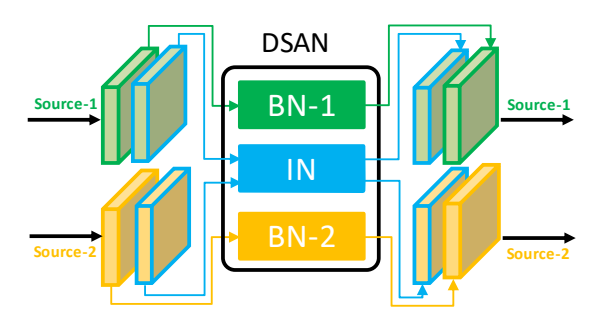


Figure 4: Illustration of the proposed DSAN. In this figure, we take two source domains as an example.

Remark. The advantage of using the DSAN to achieve the DSAF has two folds. Firstly, DSAN can simultaneously tackle the inter-domain interference during pseudo-labeling and domain gap between source domains and unseen target domain. Secondly, using the DSAN merely adds a small number of parameters in the model due to sharing all layers except for the normalization layer. It is worth noting that DSAN is not the unique method to implement DSAF, thus DSAF could be implemented via other methods.

Although the DSAF needs to add a new path for each new dataset, the number of the added parameter in a new path is extremely small because the method only changes the normalization layer of the baseline. Here, we show the memory size of our method (30190MB) and the baseline (30014MB) when using two datasets in the training stage. As seen, our method does not add a large memory size.

3.4. Details of Network Framework

In this paper, we use ResNet-50 [60] as backbone, which mainly consists of four blocks. We employ our proposed DSAN in all blocks by replacing the original BN. Besides, for generating the pseudo-labels, we utilize DBSCAN [61] to conduct the clustering after each epoch. Based on these pseudo-labels, we directly employ the cross-entropy loss (\mathcal{L}_{cls}) and triplet loss (\mathcal{L}_{tri}) with hard sample mining [62, 63, 64] to train the model as below:

$$\mathcal{L}_{total} = \mathcal{L}_{cls} + \mathcal{L}_{tri}. \tag{8}$$

In the testing stage, since our method for each source domain has an independent path, the features from all paths are averaged as the final feature.

Remark. Our method can also be used into the supervised DG-ReID case when given the label information of all sources. Using the domain-specific framework could extract the features of the unseen target domain from the different views because different domain-specific paths map the same sample into different spaces, and features from different domain paths could be complementary. Therefore, the fused features also bring the good performance in the supervised case, which will be verified in the experiment.

Besides, our method is designed for the "A+B \rightarrow C" task, where "A", "B" and "C" denote different domains, and there are no available labels in "A" and "B". Thus, we can directly convert the original task to the "A+B \rightarrow A, B" task, which is similar to the UDA task, yet removing the labels of the source domain during training. We call this task as UDAw/oSL (*i.e.*, UDA without source labels). Particularly, if using our method to solve this UDAw/oSL task, we can obtain the competitive results when compared to the strong UDA-ReID baselines, as validated in the experiment.

4. Experiments

In this part, we firstly introduce the experimental datasets and settings in Section 4.1. Then, we compare the proposed method with the basic networks in Section 4.2, respectively. To validate the effectiveness of various components in the pro-

posed framework, we conduct ablation studies in Section 4.3. Besides, we further analyze the property of the proposed method in Section 4.4. In Section 4.5, we also validate the effectiveness of our method in the supervised DG-ReID. Lastly, we convert UDG-ReID to the UDAw/oSL-ReID task in Section 4.6, which shows the non-necessity of source labels in the typical UDA-ReID task.

4.1. Dataset and Setting

Datasets. We evaluate our method on three large-scale image datasets: Market1501 (Ma) [65], DukeMTMC-reID (D) [66], MSMT17 (Ms) [67], and CUHK03-NP (C) [68, 69]. The partition of training and testing sets on each dataset is the same as [26]. Market1501 (Ma) contains 1,501 persons with 32,668 images from six cameras. Among them, 12,936 images of 751 identities are used as training set. For evaluation, there are 3,368 and 19,732 images in the query set and the gallery set, respectively. **DukeMTMC-reID** (**D**) has 1,404 persons from eight cameras, with 16, 522 training images, 2, 228 queries, and 17, 661 gallery images. MSMT17 (Ms) is collected from a 15-camera network deployed on campus. The training set contains 32,621 images of 1,041 identities. For evaluation, 11,659 and 82,161 images are adopted as query and gallery images, respectively. CUHK03-NP (C) has an average of 4.8 images in each camera. The dataset provides both manually labeled bounding boxes and DPM-detected bounding boxes. The dataset provides both manually labeled bounding boxes and DPM-detected bounding boxes. On this dataset, there are 7,365 training images, and 1,400 images and 5,332 images in query set and gallery set are used in the testing stage. For all datasets, we employ CMC accuracy and mAP for ReID evaluation [65, 70].

Implementation Details. In this experiment, we use the pre-trained ResNet-50 on ImageNet [71] to initialize the network parameters. In a batch, the number of IDs and the number of images per person are set as 16 and 4 to produce triplets, respectively. The learning rate is 3.5×10^{-4} . The proposed model is trained with the Adam optimizer in a total of 50 epochs. The size of the input image is 256×128 . For data augmentation, we merely perform random cropping and random flipping. Similar to [24], we do not utilize random erasing because it will degenerate the cross-domain ReID performance.

Table 2: Experimental results of different methods on Market1501, DukeMTMC-reID and MSMT17. "Supervised" denotes giving all source labels for our method (DSAF). The bold is the best result.

	Market+Duke→MSMT					
Method	mAP Rank-1 Ra		Rank-5	Rank-10		
Baseline	3.7	11.6	19.5	23.5		
IBN-Net [59]	5.7	17.4	26.7	31.8		
DSAF	10.3	28.9	39.9	45.5		
Supervised	11.7	31.1	43.3	48.9		
	Market+MSMT→Duke					
Baseline	15.3	26.6	41.9	48.3		
IBN-Net [59]	18.2	34.1	49.4	55.9		
DSAF	39.9	61.3	73.4	77.5		
Supervised	44.3	63.7	76.1	80.4		
		Duke+MS	SMT→Maı	rket		
Baseline	21.3	47.0	64.1	70.9		
IBN-Net [59]	25.5	54.1	69.9	76.5		
DSAF	37.6	68.2	81.4	86.4		
Supervised	40.9	70.9	83.9	88.1		

In all experiments, the "Baseline" denotes using the raw ResNet-50 [60] in Fig. 2. Particularly, all experiments on all datasets utilize the same setting.

4.2. Comparison with Basic Networks

In this part, we conduct the experiment to compare our method with some basic networks, *e.g.*, ResNet-50 [60] and IBN-Net [59], as reported in Tab. 2. As seen, IBN-Net outperforms the baseline (*i.e.*, ResNet-50) model, which mainly thanks to the IN structure in the network, thus it can reach better generalization ability in the unseen target domain. Besides, our method can achieve better performance than other methods. For example, compared to IBN-Net, in the "Duke+MSMT \rightarrow Market" task, our method improves mAP and Rank-1 by +12.1% (37.6 vs. 25.5) and +14.1% (68.2 vs. 54.1). This main reason is that, in the UDG-ReID task we need to simultaneously

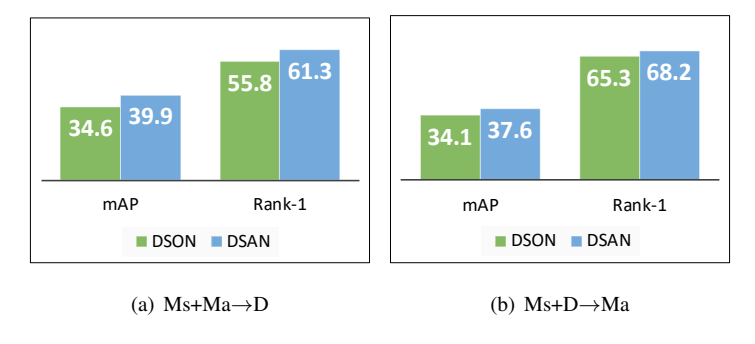


Figure 5: Comparison between DSAN and DSON [36].

solve the domain interference during pseudo-labeling and the generalization issue in unseen target domains. However, IBN-Net merely considers IN to deal with the latter issue.

Moreover, we report the experimental results of our method when giving the labels for all training samples. As seen in Tab. 2, our method in the UDG-ReID task slightly drops when compared to the supervised DG setting. Particularly, our method in the supervised DG setting also can achieve competitive performance when compared to some SOTA methods, as shown in Sec. 4.5.

In addition, we also compare the proposed DSAN with DSON [36], which utilizes the domain-specific normalization technique for the supervised DG classification task, and it can also be employed to implement our DSAF. DSON conducts the fusion of the batch and instance statistics and then performs the normalization, which could be not robust for the unseen domains due to the inaccurate pseudo-labels of source domains in our unsupervised DG-ReID. As seen in Fig. 5, our DSAN can outperform the DSON.

4.3. Ablation Study

In this part, we conduct the ablation study to validate the effectiveness of each component of our method, as reported in Tab. 3. Firstly, based on the baseline model (*i.e.*, the original ResNet-50), we employ the domain-specific normalization (DSBN) to alleviate the inter-domain interference, which can produce the more reliable pseudo-labels for unlabeled data. As seen in Tab. 3, using DSBN indeed brings the improvement of performance in the target domain. Secondly, when we add the proposed DSAN into

Table 3: Ablation study on Market1501, DukeMTMC-reID and MSMT17. Note the bold is the best result.

	Market+Duke→MSMT						
Method	mAP	Rank-1	Rank-5	Rank-10			
Baseline	3.7	11.6	19.5	23.5			
+DSBN	6.3	19.4	28.8	33.5			
+DSAN	10.3	28.9	39.9	45.5			
	Market+MSMT→Duke						
Baseline	15.3	26.6	41.9	48.3			
+DSBN	30.6	49.8	64.6	69.3			
+DSAN	39.9	61.3	73.4	77.5			
	Duke+MSMT→Market						
Baseline	21.3	47.0	64.1	70.9			
+DSBN	29.9	60.7	75.8	81.1			
+DSAN	37.6	68.2	81.4	86.4			

the above model, the mAP and Rank can be further boosted, which mainly owes to the generalization ability of IN in the proposed DSAN. In the "Market+MSMT \rightarrow Duke" task, our DSAN can increase +9.3% (39.9 vs. 30.6) and +11.5% (61.3 and 49.8) on mAP and Rank-1, respectively.

Besides, we validate the necessity of the affine transformation of IN in DSAN, *i.e.*, γ^{in} , β^{in} in Eq. (1), as reported in Tab. 4. As seen, if we remove the affine operation, the performance will have a large degradation, because using affine could make the feature maps of IN suitable for another half the feature maps of BN. Moreover, we verify the effectiveness of sharing affine of IN for all source domains. As seen in Tab. 4, sharing affine operation can obtain better experimental results in the unseen target domains, and it is used in our all experiments. For example, in the "Market+MSMT \rightarrow Duke" task, using the independent affine operation of IN for each domain in DSAN will decrease -1.7% (38.2 vs. 39.9) and -1.5% (59.8 vs. 61.3) on mAP and Rank-1 when compared with the model using shared affine operation for all domains. This main reason is that, if we leverage the independent affine operation for each source domain, it could cause

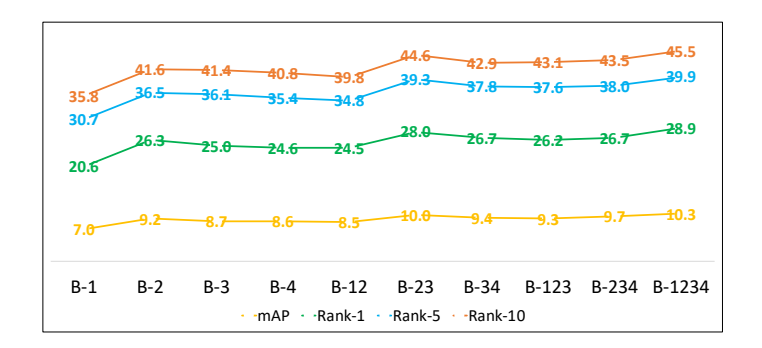


Figure 6: Results of different positions of DSAN in the backbone in the "Market+Duke→MSMT" task. "B-123" denotes that we use the DSAN in Block 1, 2 and 3 of ResNet-50.

that the learnable affine sightly overfits to the corresponding domain.

4.4. Further Analysis

Evaluation on the policy of splitting the channels into two parts. We conduct the experiment of different policies on splitting the channels into two parts, as listed in Tab. 5. We split the channel into 25% (50%, or 75%) IN and 75% (50%, or 25%) BN. As seen, when we split the channel into 50% IN and 50% BN, the performance is best, which reveals that the domain-specific information based on BN and sample-specific information based on IN is equally important in our task. In our all experiments, we split the channel into 50% IN and 50% BN.

Evaluation on the position of DSAN. As known, ResNet-50 mainly consists of four blocks [60]. Here, we evaluate the impact of the different positions of DSAN in the backbone, as shown in Fig. 6. Compared to the baseline method in the "Market+Duke→MSMT" task as shown in Tab. 3 (*i.e.*, mAP=3.7% and Rank-1=11.6%), the proposed DSAN used in any position can reach the better performance. Besides, we observe that, if using DSAN in a Block, the model with DSAN in Block 2 has better results than the model with DSAN in other Blocks. Moreover, when we use the proposed DSAN in all Blocks of the backbone, the best results can be yielded. In particular, using DSAN does not bring more parameters than the original ResNet-50. In our experiment, we use the same setting in all tasks.

Evaluation on more source domains. We evaluate our method in more source

Table 4: Experimental results with or without affine of IN in DSAN. "Share" denotes that if sharing the affine for each source domains. " \checkmark - \checkmark " is that DSAN includes the affine of IN and shares the unique affine for each domains in the training stage.

	Duke+MSMT→Market					
Affine-Share	mAP	mAP Rank-1 F		Rank-10		
X- X	28.6	57.6	73.9	79.4		
√ - X	36.4	67.3	80.7	85.5		
✓ - ✓	37.6	68.2	81.4	86.4		
	Market+MSMT→Duke					
X- X	25.8	43.4	57.9	63.8		
√ - X	38.2 59.8 71.9			77.0		
√ - √	39.9	61.3	73.4	77.5		
	Market+Duke→MSMT					
X- X	6.0	18.1	27.4	32.4		
√ - X	9.7	27.8	39.3	44.9		
√ - √	10.3	28.9	39.9	45.5		

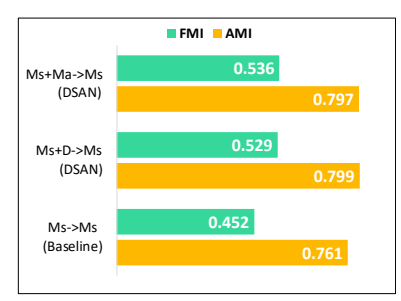
domains, as reported in Tab. 6. As seen, the model trained via three source domains can obtain better performance than the model trained with two source domains. For example, the mAP and Rank-1 of the model in the Ma+D+Ms→C task outperform the model in the "Ma+Ms→C" task by +2.1% (17.0 vs. 14.9) and +2.0% (16.9 vs. 14.9). This shows that our method can also effectively alleviate the interference of the domain gap across different domains when there are more available unlabeled source domains in the training stage.

Evaluation on the pseudo-label quality. As aforementioned, if we use the conventional baseline method to conduct the proposed UDG-ReID, it will produce poor pseudo-labels for the unlabeled training domains due to the domain-shift between different source domains. In this part, we validate the efficacy of our method from two different perspectives, including performance and clustering accuracy in the source domains, as shown in Tab. 7 and Fig. 7. Firstly, as seen in Tab. 7, our method can produce

Table 5: Experimental results of different policies on splitting the channels into two parts. In this table, we conduct an experiment on Market, Duke and MSMT. We use two datasets to train the model and test the remaining dataset. For example, "Market" denotes that the model is trained on MSMT and Duke and tested on Market.

		Market		Duke		MSMT	
IN	BN	mAP	Rank-1	mAP	Rank-1	mAP	Rank-1
0.25	0.75	36.3	67.1	36.6	56.3	9.3	26.2
0.75	0.25	36.3	65.6	38.5	58.3	10.3	28.2
0.50	0.50	37.6	68.2	39.9	61.3	10.3	28.9





(a) Performance

(b) Clustering evaluation

Figure 7: Performance and clustering results on MSMT17. As seen in this figure, our method can effectively mitigate the existing issue as shown in Fig. 3.

better results than the baseline method, and the clustering accuracy is higher than the baseline. In the "Duke+MSMT→Market" task, the mAP and Rank-1 can improve +17% (27.2 vs. 10.2) and +31.0% (57.5 vs. 26.5), and AMI and FMI can increase +0.142 (0.799 vs. 0.657) and +0.229 (0.529 vs. 0.300). This confirms that our method can alleviate the inter-domain interference during generating pseudo-labels so as to yield more reliable pseudo-labels to train the model.

Moreover, we also compare our method with the model trained in a single domain. If we utilize multiple domains to train the baseline model, it will result in poor performance when compared to employing a single domain to train the model, as shown in Fig. 3. Differently, as seen in Fig. 7, our method can alleviate the issue, and can fully exploit each domain to boost the discrimination of the model.

Table 6: Experimental results of the model trained using different numbers of source domains and tested on CUHK03-NP.

Setting	mAP	Rank-1	Rank-5	Rank-10
Ma+D→C	12.7	13.1	23.8	29.9
$D+Ms \rightarrow C$	12.1	12.1	21.6	27.7
$Ma+Ms \rightarrow C$	14.9	14.9	27.1	34.8
$Ma+D+Ms \rightarrow C$	17.0	16.9	29.3	37.3

Table 7: Experimental results and clustering accuracy of source domains in different tasks. AMI (Adjusted Mutual Information) and FMI (Fowlkes-Mallows Index) are two clustering evaluation protocols, and the larger value is better.

		Train: Market + Duke										
Method			Test:	Market					Test:	Duke		
	mAP	rank-1	rank-5	rank-10	AMI	FMI	mAP	Rank-1	Rank-5	Rank-10	AMI	FMI
Baseline	48.1	72.1	86.6	90.4	0.781	0.449	41.0	57.7	71.8	76.7	0.796	0.508
DSAF	69.9	88.7	95.0	96.5	0.874	0.646	55.7	73.8	83.9	87.5	0.845	0.585
	Train: Market + MSMT											
			Test:	Market			Test: MSMT					
Baseline	44.4	69.8	84.5	89.4	0.773	0.464	8.4	22.5	32.9	37.7	0.627	0.242
DSAF	72.8	89.5	95.8	97.4	0.886	0.689	26.5	56.7	68.7	73.6	0.797	0.536
					Т	rain: Du	ke + MS	SMT				
	Test: Duke					Test: N	MSMT					
Baseline	39.2	56.9	72.1	77.1	0.795	0.516	10.2	26.5	38.0	43.5	0.657	0.300
DSAF	59.0	76.0	85.0	88.2	0.846	0.582	27.2	57.5	69.3	73.8	0.799	0.529

Effectiveness of feature fusion in the testing stage. Since our DSAN uses the independent BN for each domain, we fuse the feature from each branch to form the final feature for testing. As seen in Tab. 8, the fused features can yield better performance than the features from the single path. For example, in the "Duke+MSMT→Market" task, using the fused feature can increase +3.1% (37.6 vs. 34.5) and +2.6% (37.6 vs. 35.0) when compared to the features from "path-duke" and "path-msmt". This main reason is that the features in each branch could be complementary due to the domain discrepancy, thus the fused features can bring further improvement of the performance. Here we also give the data distribution from each path, as shown in Fig. 8. As seen, the features extracted by different paths are scattered. Thus, features of different domain-

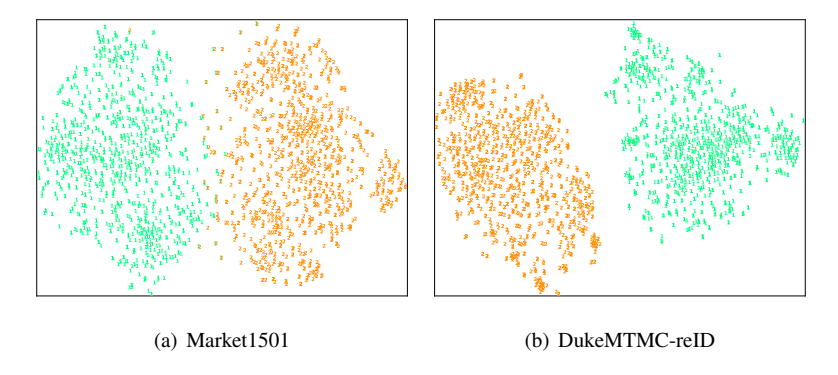


Figure 8: Visualization of features from different paths of our model via t-SNE [72] on Market1501 and DukeMTMC-reID, which corresponds to the "Duke+MSMT→Market" and "Market+MSMT→Duke" tasks. Note that, in each figure, different colors denote that the same samples from the same dataset pass different paths.

paths might be complementary, and fused features are more discriminative.

4.5. Extension to Supervised DG-ReID Case

In this experiment, we also use our method under the supervised DG person ReID, and compare it with the recent DG-ReID methods, such as QAConv50 and M³L, as reported in Tab. 9. QAConv50 [27] treats image matching as finding local correspondences in feature maps, and constructs query-adaptive convolution kernels on the fly to achieve local matching. M³L [26] introduces a meta-learning strategy to simulate the train-test process of domain generalization for learning more generalizable models, the memory-based identification loss to overcome the unstable meta-optimization caused by the parametric classifier, and a meta batch normalization layer to diversify meta-test features. As seen in Tab. 9, our method outperforms these methods, despite our method being very simple. Particularly, on the large-scale dataset (MSMT17), the Rank-1 of our method improves the results of M³L by +5.3% (42.4 vs. 37.1), which owes to the generalization capability of the fused features, as reported in Tab. 9.

4.6. UDA-ReID without Source Labels

As mentioned in Sec. 3.4, the proposed UDG-ReID task can be converted to the UDAw/oSL-ReID task, which equals to the case that UDA removes labels from the

Table 8: Comparison of the domain-path feature and the fused feature. "Path-duke" is the feature from Duke-path.

	Market+Duke→MSMT					
Method	mAP	Rank-1	Rank-5	Rank-10		
Path-market	8.8	25.0	36.4	41.8		
Path-duke	9.4	27.3	38.5	43.9		
Fusion	10.3	28.9	39.9	45.5		
	Market+MSMT→Duke					
Path-market	32.5	52.9	67.6	72.5		
Path-msmt	38.3	60.5	72.9	76.8		
Fusion	39.9	61.3	73.4	77.5		
		Duke+MS	MT→Maı	rket		
Path-duke	35.0	65.4	79.4	85.2		
Path-msmt	34.5	65.1	79.2	84.5		
Fusion	37.6	68.2	81.4	86.4		

Table 9: Experimental results under the supervised DG setting. When we evaluates models on Market1501 (or MSMT17), "DSAF-P1", "DSAF-P2" and "DSAF-P3" indicate using the features from the Path-Duke, Path-MSMT17 and Path-CUHK03 (or Path-Market, Path-Duke and Path-CUHK03), respectively.

	D+Ms	+C→Ma	$Ma+D+C \rightarrow Ms$		
Method	mAP	Rank-1	mAP	Rank-1	
QAConv50 [27]	39.5	68.6	10.0	29.0	
M ³ L(ResNet50) [26]	51.1	76.5	13.1	32.0	
M ³ L(IBN-Net50) [26]	52.5	78.3	15.4	37.1	
DSAF-P1	44.4	73.6	10.8	29.7	
DSAF-P2	45.3	73.5	14.9	39.3	
DSAF-P3	44.2	72.7	9.8	29.7	
DSAF (ours)	53.2	79.7	16.8	42.4	

source domain. The UDAw/oSL-ReID task does not need to annotate the originally collected data, thus it is more valuable than the UDA task in the real-world application. We conduct the experiment to compare our method in the UDAw/oSL-ReID task with strong UDA-ReID baselines, such as SBase-1 [46] and SBase-2 [73], as reported in Tab. 10. Particularly, in this experiment, we add the random erasing data augmentation [74] to enrich the diversity of samples due to no domain gap between the training set and the testing set, which is also used in SBase-1 [46] and SBase-2 [75]. Besides, SBase-1 utilizes contrastive loss across memory bank [76] and mean teacher method [77], and SBase-2 [73] uses XBM to mine more hard negatives for the triplet loss, which is a variant of the memory bank. Differently, our method does not leverage these above operations. As seen in Tab. 10, although there is no available label information in the source domain, the UDAw/oSL-ReID task with our method can obtain competitive results when compared to strong baseline UDA methods. Furthermore, we also conduct the UDA case with our method, and the results are also similar to the UDAw/oSL-ReID case. This means that removing the labels from the source domain does not bring the largely negative impact in the UDA task. Thus, the UDAw/oSL-ReID might be more valuable than the UDA-ReID in future ReID community.

Table 10: Experimental results of different methods in the UDA-ReID task and the UDAw/oSL-ReID task, respectively.

	Ma+	D→Ma	Ma+D→D		
Task	mAP	Rank-1	mAP	Rank-1	
UDA(SBase-1) [46]	75.4	89.8	64.8	79.7	
UDA(SBase-2) [73]	79.1	91.2	65.8	80.1	
UDA(DSAF)	78.6	91.7	65.2	80.1	
UDAw/oSL(DSAF)	78.5	91.0	64.2	78.6	

5. Conclusion

This paper proposes an unsupervised DG-ReID task, where there is no available label information in all source domains. It is more challenging than the typical DG

person ReID task. Considering there exist two problems in the task, including the inter-domain interference during pseudo-labeling and the domain discrepancy between the source and target domains, we propose a unified method to simultaneously solve the two issues, called domain-specific adaptive framework (DSAF), which can reduce the impact of domain interference to produce the reliable pseudo-labels and enhance the robustness of the model in the unseen domain. We conduct extensive experiments on multiple benchmark datasets to confirm the efficacy of the proposed method. Moreover, we convert the UDG-ReID task to the UDAw/oSL-ReID task, which can obtain the competitive results using our method when compared to the strong UDA-ReID baselines.

6. Acknowledgment

This work was supported by NSFC Program (62206052, 62125602, 62076063, 62222604), CAAI-Huawei MindSpore Project (CAAIXSJLJJ-2021-042A), China Postdoctoral Science Foundation Project (2021M690609), Jiangsu Natural Science Foundation Project (BK20210224), and CCF-Lenovo Bule Ocean Research Fund.

References

- [1] M. Ye, J. Shen, G. Lin, T. Xiang, L. Shao, S. C. H. Hoi, Deep learning for person re-identification: A survey and outlook, arXiv preprint arXiv:2001.04193.
- [2] L. Qi, L. Wang, J. Huo, Y. Shi, X. Geng, Y. Gao, Adversarial camera alignment network for unsupervised cross-camera person re-identification, IEEE Transactions on Circuits and Systems for Video Technology (TCSVT).
- [3] L. Zheng, Y. Yang, A. G. Hauptmann, Person re-identification: Past, present and future, arXiv preprint arXiv:1610.02984.
- [4] L. Qi, L. Wang, J. Huo, Y. Shi, Y. Gao, Progressive cross-camera soft-label learning for semi-supervised person re-identification, IEEE Transactions on Circuits and Systems for Video Technology (TCSVT) 30 (9) (2020) 2815–2829.

- [5] Y. Sun, L. Zheng, Y. Yang, Q. Tian, S. Wang, Beyond part models: Person retrieval with refined part pooling (and A strong convolutional baseline), in: European Conference on Computer Vision (ECCV), 2018, pp. 501–518.
- [6] Z. Dai, M. Chen, X. Gu, S. Zhu, P. Tan, Batch dropblock network for person re-identification and beyond, in: International Conference on Computer Vision (ICCV), 2019, pp. 3690–3700.
- [7] K. Zhou, Y. Yang, A. Cavallaro, T. Xiang, Omni-scale feature learning for person re-identification, in: International Conference on Computer Vision (ICCV), 2019, pp. 3701–3711.
- [8] M. Zheng, S. Karanam, Z. Wu, R. J. Radke, Re-identification with consistent attentive siamese networks, in: IEEE Conference on Computer Vision and Pattern Recognition (CVPR), 2019, pp. 5735–5744.
- [9] D. Tao, Y. Guo, B. Yu, J. Pang, Z. Yu, Deep multi-view feature learning for person re-identification, IEEE Transactions on Circuits and Systems for Video Technology (TCSVT) 28 (10) (2017) 2657–2666.
- [10] J. Sun, Y. Li, H. Chen, B. Zhang, J. Zhu, MEMF: multi-level-attention embedding and multi-layer-feature fusion model for person re-identification, Pattern Recognition (PR) 116 (2021) 107937.
- [11] W. Wu, D. Tao, H. Li, Z. Yang, J. Cheng, Deep features for person reidentification on metric learning, Pattern Recognition (PR) 110 (2021) 107424.
- [12] L. Qi, L. Wang, J. Huo, L. Zhou, Y. Shi, Y. Gao, A novel unsupervised cameraaware domain adaptation framework for person re-identification, in: International Conference on Computer Vision (ICCV), 2019, pp. 8079–8088.
- [13] A. Wu, W. Zheng, J. Lai, Unsupervised person re-identification by camera-aware similarity consistency learning, in: International Conference on Computer Vision (ICCV), 2019, pp. 6921–6930.

- [14] H. Yu, W. Zheng, A. Wu, X. Guo, S. Gong, J. Lai, Unsupervised person reidentification by soft multilabel learning, in: IEEE Conference on Computer Vision and Pattern Recognition (CVPR), 2019, pp. 2148–2157.
- [15] Y. Zhai, S. Lu, Q. Ye, X. Shan, J. Chen, R. Ji, Y. Tian, Ad-cluster: Augmented discriminative clustering for domain adaptive person re-identification, in: IEEE Conference on Computer Vision and Pattern Recognition (CVPR), 2020, pp. 9018–9027.
- [16] S. Bak, P. Carr, J. Lalonde, Domain adaptation through synthesis for unsupervised person re-identification, in: European Conference on Computer Vision (ECCV), 2018, pp. 193–209.
- [17] H. Feng, M. Chen, J. Hu, D. Shen, H. Liu, D. Cai, Complementary pseudo labels for unsupervised domain adaptation on person re-identification, IEEE Transactions on Image Processing (TIP) 30 (2021) 2898–2907.
- [18] H. Li, Y. Chen, D. Tao, Z. Yu, G. Qi, Attribute-aligned domain-invariant feature learning for unsupervised domain adaptation person re-identification, IEEE Transactions on Information Forensics and Security (TIFS) 16 (2021) 1480–1494.
- [19] P. Peng, T. Xiang, Y. Wang, M. Pontil, S. Gong, T. Huang, Y. Tian, Unsupervised cross-dataset transfer learning for person re-identification, in: IEEE Conference on Computer Vision and Pattern Recognition (CVPR), 2016, pp. 1306–1315.
- [20] J. Song, Y. Yang, Y. Song, T. Xiang, T. M. Hospedales, Generalizable person re-identification by domain-invariant mapping network, in: IEEE Conference on Computer Vision and Pattern Recognition (CVPR), 2019, pp. 719–728.
- [21] S. Choi, T. Kim, M. Jeong, H. Park, C. Kim, Meta batch-instance normalization for generalizable person re-identification, in: IEEE Conference on Computer Vision and Pattern Recognition (CVPR), 2021, pp. 3425–3435.
- [22] Y. Dai, X. Li, J. Liu, Z. Tong, L. Duan, Generalizable person re-identification with relevance-aware mixture of experts, in: IEEE Conference on Computer Vision and Pattern Recognition (CVPR), 2021, pp. 16145–16154.

- [23] J. Jia, Q. Ruan, T. M. Hospedales, Frustratingly easy person re-identification: Generalizing person re-id in practice, in: British Machine Vision Conference (BMVC), 2019, p. 117.
- [24] X. Jin, C. Lan, W. Zeng, Z. Chen, L. Zhang, Style normalization and restitution for generalizable person re-identification, in: IEEE Conference on Computer Vision and Pattern Recognition (CVPR), 2020, pp. 3140–3149.
- [25] D. Ulyanov, A. Vedaldi, V. Lempitsky, Instance normalization: The missing ingredient for fast stylization, arXiv preprint arXiv:1607.08022.
- [26] Y. Zhao, Z. Zhong, F. Yang, Z. Luo, Y. Lin, S. Li, N. Sebe, Learning to generalize unseen domains via memory-based multi-source meta-learning for person re-identification, in: IEEE Conference on Computer Vision and Pattern Recognition (CVPR), 2021, pp. 6277–6286.
- [27] S. Liao, L. Shao, Interpretable and generalizable person re-identification with query-adaptive convolution and temporal lifting, in: European Conference on Computer Vision (ECCV), 2020, pp. 456–474.
- [28] K. Zhou, Y. Yang, T. M. Hospedales, T. Xiang, Learning to generate novel domains for domain generalization, in: European Conference on Computer Vision (ECCV), 2020, pp. 561–578.
- [29] K. Zhou, Y. Yang, Y. Qiao, T. Xiang, Domain generalization with mixstyle, in: International Conference on Learning Representations (ICLR), 2021.
- [30] Z. Huang, H. Wang, E. P. Xing, D. Huang, Self-challenging improves cross-domain generalization, in: European Conference on Computer Vision (ECCV), 2020, pp. 124–140.
- [31] K. Zhou, Y. Yang, T. M. Hospedales, T. Xiang, Deep domain-adversarial image generation for domain generalisation, in: AAAI Conference on Artificial Intelligence (AAAI), 2020, pp. 13025–13032.

- [32] P. Li, D. Li, W. Li, S. Gong, Y. Fu, T. M. Hospedales, A simple feature augmentation for domain generalization, in: International Conference on Computer Vision (ICCV), 2021, pp. 8886–8895.
- [33] J. Zhang, L. Qi, Y. Shi, Y. Gao, Generalizable model-agnostic semantic segmentation via target-specific normalization, Pattern Recognition (PR) 122 (2022) 108292.
- [34] H. Nam, H. Lee, J. Park, W. Yoon, D. Yoo, Reducing domain gap by reducing style bias, in: IEEE Conference on Computer Vision and Pattern Recognition (CVPR), 2021, pp. 8690–8699.
- [35] Q. Xu, R. Zhang, Y. Zhang, Y. Wang, Q. Tian, A fourier-based framework for domain generalization, in: IEEE Conference on Computer Vision and Pattern Recognition (CVPR), 2021, pp. 14383–14392.
- [36] S. Seo, Y. Suh, D. Kim, G. Kim, J. Han, B. Han, Learning to optimize domain specific normalization for domain generalization, in: European Conference on Computer Vision (ECCV), 2020, pp. 68–83.
- [37] C. Luo, C. Song, Z. Zhang, Generalizing person re-identification by cameraaware invariance learning and cross-domain mixup, in: European Conference on Computer Vision (ECCV), 2020, pp. 224–241.
- [38] X. Jin, C. Lan, W. Zeng, Z. Chen, Global distance-distributions separation for unsupervised person re-identification, in: European Conference on Computer Vision (ECCV), 2020, pp. 735–751.
- [39] G. Chen, Y. Lu, J. Lu, J. Zhou, Deep credible metric learning for unsupervised domain adaptation person re-identification, in: European Conference on Computer Vision (ECCV), 2020, pp. 643–659.
- [40] Y. Lin, L. Xie, Y. Wu, C. Yan, Q. Tian, Unsupervised person re-identification via softened similarity learning, in: IEEE Conference on Computer Vision and Pattern Recognition (CVPR), 2020, pp. 3387–3396.

- [41] F. Yang, K. Yan, S. Lu, H. Jia, D. Xie, Z. Yu, X. Guo, F. Huang, W. Gao, Partaware progressive unsupervised domain adaptation for person re-identification, IEEE Transactions on Multimedia (TMM) 23 (2021) 1681–1695.
- [42] Y. Bai, C. Wang, Y. Lou, J. Liu, L. Duan, Hierarchical connectivity-centered clustering for unsupervised domain adaptation on person re-identification, IEEE Transactions on Image Processing (TIP) 30 (2021) 6715–6729.
- [43] C. Zhang, Y. Tang, Z. Zhang, D. Li, X. Yang, W. Zhang, Improving domain-adaptive person re-identification by dual-alignment learning with camera-aware image generation, IEEE Transactions on Circuits and Systems for Video Technology (TCSVT) 31 (11) (2020) 4334–4346.
- [44] D. Zheng, J. Xiao, K. Chen, X. Huang, L. Chen, Y. Zhao, Soft pseudo-label shrinkage for unsupervised domain adaptive person re-identification, Pattern Recognition (PR) 127 (2022) 108615.
- [45] F. Yang, Z. Zhong, Z. Luo, Y. Cai, Y. Lin, S. Li, N. Sebe, Joint noise-tolerant learning and meta camera shift adaptation for unsupervised person re-identification, in: IEEE Conference on Computer Vision and Pattern Recognition (CVPR), 2021, pp. 4855–4864.
- [46] K. Zheng, C. Lan, W. Zeng, Z. Zhang, Z. Zha, Exploiting sample uncertainty for domain adaptive person re-identification, in: AAAI Conference on Artificial Intelligence (AAAI), 2021, pp. 3538–3546.
- [47] Y. Ge, D. Chen, H. Li, Mutual mean-teaching: Pseudo label refinery for unsupervised domain adaptation on person re-identification, in: International Conference on Learning Representations (ICLR), 2020.
- [48] K. Zheng, W. Liu, L. He, T. Mei, J. Luo, Z. Zha, Group-aware label transfer for domain adaptive person re-identification, in: IEEE Conference on Computer Vision and Pattern Recognition (CVPR), 2021, pp. 5310–5319.

- [49] S. Xuan, S. Zhang, Intra-inter camera similarity for unsupervised person reidentification, in: IEEE Conference on Computer Vision and Pattern Recognition (CVPR), 2021, pp. 11926–11935.
- [50] Y. Ge, F. Zhu, D. Chen, R. Zhao, H. Li, Self-paced contrastive learning with hybrid memory for domain adaptive object re-id, in: Advances in Neural Information Processing Systems (NeurIPS), 2020.
- [51] Z. Bai, Z. Wang, J. Wang, D. Hu, E. Ding, Unsupervised multi-source domain adaptation for person re-identification, in: IEEE Conference on Computer Vision and Pattern Recognition (CVPR), 2021, pp. 12914–12923.
- [52] X. Zhang, L. Zhou, R. Xu, P. Cui, Z. Shen, H. Liu, Domain-irrelevant representation learning for unsupervised domain generalization, arXiv preprint arXiv:2107.06219.
- [53] T. Chen, S. Kornblith, M. Norouzi, G. E. Hinton, A simple framework for contrastive learning of visual representations, in: International Conference on Machine Learning (ICML), 2020, pp. 1597–1607.
- [54] K. He, H. Fan, Y. Wu, S. Xie, R. B. Girshick, Momentum contrast for unsupervised visual representation learning, in: IEEE Conference on Computer Vision and Pattern Recognition (CVPR), 2020, pp. 9726–9735.
- [55] G. M. Van de Ven, A. S. Tolias, Three scenarios for continual learning, arXiv preprint arXiv:1904.07734.
- [56] Y. Yang, D.-W. Zhou, D.-C. Zhan, H. Xiong, Y. Jiang, Adaptive deep models for incremental learning: Considering capacity scalability and sustainability, in: ACM International Conference on Knowledge Discovery & Data Mining (SIGKDD), 2019, pp. 74–82.
- [57] X. V. Nguyen, J. Epps, J. Bailey, Information theoretic measures for clusterings comparison: Variants, properties, normalization and correction for chance, Journal of Machine Learning Research (JMLR) 11 (2010) 2837–2854.

- [58] W. Chang, T. You, S. Seo, S. Kwak, B. Han, Domain-specific batch normalization for unsupervised domain adaptation, in: IEEE Conference on Computer Vision and Pattern Recognition (CVPR), 2019, pp. 7354–7362.
- [59] X. Pan, P. Luo, J. Shi, X. Tang, Two at once: Enhancing learning and generalization capacities via ibn-net, in: European Conference on Computer Vision (ECCV), 2018, pp. 484–500.
- [60] K. He, X. Zhang, S. Ren, J. Sun, Deep residual learning for image recognition, in: IEEE Conference on Computer Vision and Pattern Recognition (CVPR), 2016, pp. 770–778.
- [61] M. Ester, H.-P. Kriegel, J. Sander, X. Xu, et al., A density-based algorithm for discovering clusters in large spatial databases with noise., in: ACM International Conference on Knowledge Discovery & Data Mining (SIGKDD), 1996, pp. 226– 231.
- [62] H. Luo, W. Jiang, Y. Gu, F. Liu, X. Liao, S. Lai, J. Gu, A strong baseline and batch normalization neck for deep person re-identification, IEEE Transactions on Multimedia (TMM) 22 (10) (2020) 2597–2609.
- [63] A. Hermans, L. Beyer, B. Leibe, In defense of the triplet loss for person reidentification, arXiv preprint arXiv:1703.07737.
- [64] Y. Fu, Y. Wei, G. Wang, Y. Zhou, H. Shi, T. S. Huang, Self-similarity grouping: A simple unsupervised cross domain adaptation approach for person reidentification, in: International Conference on Computer Vision (ICCV), 2019, pp. 6111–6120.
- [65] L. Zheng, L. Shen, L. Tian, S. Wang, J. Wang, Q. Tian, Scalable person reidentification: A benchmark, in: International Conference on Computer Vision (ICCV), 2015, pp. 1116–1124.
- [66] Z. Zheng, L. Zheng, Y. Yang, Unlabeled samples generated by GAN improve the person re-identification baseline in vitro, in: International Conference on Computer Vision (ICCV), 2017, pp. 3774–3782.

- [67] L. Wei, S. Zhang, W. Gao, Q. Tian, Person transfer GAN to bridge domain gap for person re-identification, in: IEEE Conference on Computer Vision and Pattern Recognition (CVPR), 2018, pp. 79–88.
- [68] Z. Zhong, L. Zheng, D. Cao, S. Li, Re-ranking person re-identification with k-reciprocal encoding, in: IEEE Conference on Computer Vision and Pattern Recognition (CVPR), 2017, pp. 3652–3661.
- [69] W. Li, R. Zhao, T. Xiao, X. Wang, Deepreid: Deep filter pairing neural network for person re-identification, in: IEEE Conference on Computer Vision and Pattern Recognition (CVPR), 2014, pp. 152–159.
- [70] M. Li, X. Zhu, S. Gong, Unsupervised tracklet person re-identification, IEEE Transactions on Pattern Analysis and Machine Intelligence (TPAMI) 42 (7) (2020) 1770–1782.
- [71] J. Deng, W. Dong, R. Socher, L. Li, K. Li, L. Fei-Fei, Imagenet: A large-scale hierarchical image database, in: IEEE Conference on Computer Vision and Pattern Recognition (CVPR), 2009, pp. 248–255.
- [72] L. Van der Maaten, G. Hinton, Visualizing data using t-sne, Journal of machine learning research (JMLR) 9 (11) (2008) 2579–2605.
- [73] Y. Dai, J. Liu, Y. Sun, Z. Tong, C. Zhang, L.-Y. Duan, Idm: An intermediate domain module for domain adaptive person re-id, in: International Conference on Computer Vision (ICCV), 2021, pp. 11864–11874.
- [74] Z. Zhong, L. Zheng, G. Kang, S. Li, Y. Yang, Random erasing data augmentation, in: AAAI Conference on Artificial Intelligence (AAAI), 2020, pp. 13001–13008.
- [75] X. Wang, H. Zhang, W. Huang, M. R. Scott, Cross-batch memory for embedding learning, in: IEEE Conference on Computer Vision and Pattern Recognition (CVPR), 2020, pp. 6387–6396.
- [76] Z. Wu, Y. Xiong, S. X. Yu, D. Lin, Unsupervised feature learning via non-parametric instance discrimination, in: IEEE Conference on Computer Vision and Pattern Recognition (CVPR), 2018, pp. 3733–3742.

[77] A. Tarvainen, H. Valpola, Mean teachers are better role models: Weight-averaged consistency targets improve semi-supervised deep learning results, in: Advances in Neural Information Processing Systems (NeurIPS), 2017, pp. 1195–1204.